Runoff Water Harvesting Optimization by Using RS, GIS and Watershed Modelling in Wadi El-Arish, Sinai

Elewa H. H.[1]
1. Water Resources Dept., National Authority for Remote Sensing & Space Sciences (NARSS), Cairo, Egypt.

Ramadan E. M.[2]
2. Water Engineering Dept., Faculty of Engineering, Zagazig University (ZU), Zagazig, Egypt.

El-Feel A. A.[3]
3. Egyptian Mineral Resources Authority (EMRA), GIS & R.S. Lab, Cairo, Egypt.

Abu El Ella E. A.[4]
4. Geology Department, Faculty of Science, Assiut University (AU), Assiut, Egypt.

Nosair A. M.[5]
5. Geology Department, Faculty of Science, Zagazig University (ZU), Zagazig, Egypt.

Abstract

Water scarcity in Sinai is the major constraint for the developmental activities. Runoff water harvesting (RWH) is one of the most effective solutions for overcoming this constraint. A peculiar approach involving the integration of geographic information systems, remote sensing and watershed modeling was followed to identify the suitable sites for implementing the runoff water harvesting constructions. Nine thematic layers, viz volume of annual flood, lineament frequency denisty, drainage frequency density, maximum flow distance, basin area, basin slope, basin length, avarage overland flow distance and soil infiltration were used as multi-decision support criteria for conducting a weighted spatial probability model to determine the potential areas for the RWH in Wadi El-Arish study area. The resultant map classified the area into three RWH potentiality classes ranging from low to high. Consequently, the suitable sites for the construction of RWH dams were determind. The map suggested the collection of runoff water at the outlets of Wadi El-Arish upstream sub-watersheds with promising runoff potentialities. These sub-watersheds are El-Bruk, Yarqa Abu Taryfya, El-Fetahay El-Aqaba and Geraia; with runoff volumes of 14,304,144 m^3/y, 42,593,062 m^3/y, 14,405,379 m^3/y, 16,066,820 m^3/y, respectively. Two RWH rock-fill dams with storage capacities of 525,000 and 250,000 m^3 were proposed. These dams will mitigate the flooding hazards frequently occurring downstream the Wadi and enhance the elderly El-Rawafaa Dam. Their design criteria and technical considerations were given. The proposed damming system will allow the installment of sustainable micro-catchment agriculture, especially during the flooding seasons and mitigate the flash floods downstream the main watershed.

Key Words: Sinai, Remote Sensing, Wadi El-Arish, Geographic Information Systems, Watershed Modeling, Runoff Water Harvesting, Runoff Water Harvesting Techniques

1. Introduction

The development of Sinai Peninsula, as a land of extreme importance to Egypt is hampered by the water resources scarcity. In the present work, remote sensing (RS), geographic information systems (GIS) and watershed modelling systems (WMS) are integrated to determine the potential areas for runoff water harvesting (RWH) and the optimum sites for implementing its suitable constructions.

In Sinai, two main water resources are available; the groundwater and surface sporadic rainfalls that causes episodic flash floods in drainage basins. The groundwater exists in a variety of water bearing formations [1], including: Precambrian crystalline basement rocks, Paleozoic sandstones, Jurassic and

Cretaceous sandstones, Fractured Eocene limestone and Miocene-Quaternary clastic sequences. Consequently, new strategies and solutions had to be undertaken in order to maintain and sustain water in both sources for different activities, especially in the remote parts of Sinai. Maximizing the RWH will have its own bearing on enhancing the groundwater recharging, raising its levels and decreasing its salinities to be appropriate for different uses.

Sinai Peninsula is located between the Mediterranean Sea to the north, Red Sea to the south and embraced between the Gulf of Suez to the west and Gulf of Aqaba to the east (Fig. 1a). Sinai has an area of 61,000 km^2 and occupies a part of the arid belt of northern Africa and southwest Asia [2]. Wadi El-Arish study area is the largest drainage basin in Sinai, where it is located between latitudes 29° 00 and 31° 10' N - 33° 05' and 34° 40' E (Fig. 1b). It debouches into the southeastern littoral zone of the Mediterranean Sea. The basin covers an area of about 20,837.07 km^2, where out of which a nearly 19,000 km^2 lies inside Sinai, while the rest area is located in El-Naqb Desert. It drains the central and northern parts of Sinai (Fig. 1b). This watershed was hydrologically sub-divided into seven sub-watersheds (Fig. 1c). The upstream tributaries of the wadi originate from El-Teeh and El-Egma Plateaux. The longest water path is 310 km starting from El-Teeh Plateau at a level of 1,626 masl and ending at El-Arish City at zero level. The wadi passes through different geological and morphological regions. It upstreams from the southern mountainous and rocky terrains of very steep slopes in the south, then goes through flat sedimentary areas in the middle, and finally ends at the sand dunes near El-Arish City in the north [3].

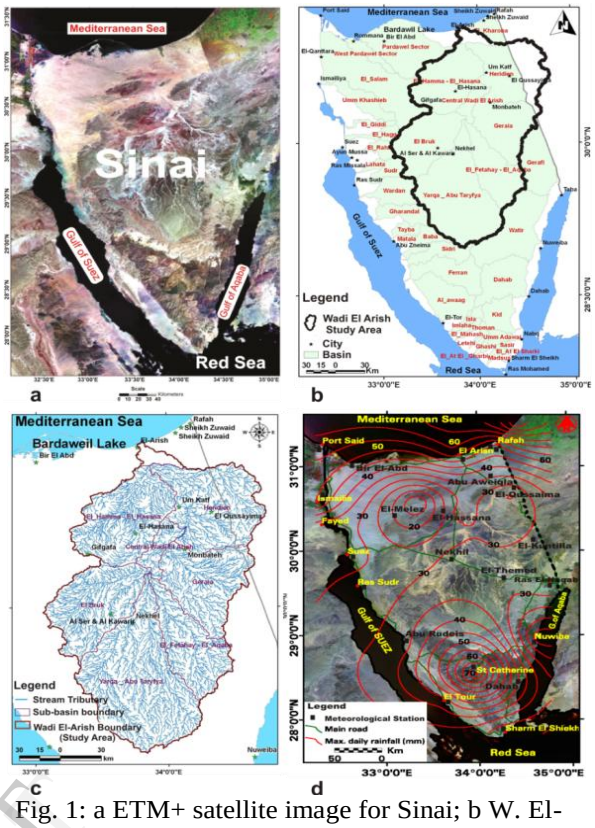

Fig. 1: a ETM+ satellite image for Sinai; b W. El-Arish study area; c Drainage net of W. El-Arish and its sub-watersheds; c Isohyetal map of Sinai

Traditional RWH had been practiced in Egypt since the Roman and Nabateen Era. Dams, basins, and cisterns are remnants from Roman times, which are frequently found in northern coastal area of Sinai [4]. Groundwater is proliferous in North Sinai, where rainfall is sufficient to recharge the Quaternary and/or even older aquifer systems. Here, RWH would be efficient and may support the installement of new settelements in the area, with a direct impact on raising the quality of life of local inhabitants [1]; [5].

The previous works proved the occurrence of promising flash floods that could economically harvest. Recharge of the alluvial aquifers flooring Wadi El-Arish in central and northern Sinai was investigated by Gheith and Sultan [6], where a hydrological model that combined the spatial and temporal distribution of rainfall, infiltration parameters, appropriate sub-basin unit hydrographs, transmission losses along stream networks and downstream runoff was developed. In their work (Op. Cit.), Wadi El-Arish watershed receives an annual average rainfall of 981.3 x 10^6 m^3 in the rainy season (November-March) of which their model indicated that 938.7 x 10^6 m^3 is the initial upstream loss, 32.5 x 10^6 m^3 is the transmission loss recharging the alluvial aquifers flooring the stream network, and 10.1 x 10^6 m^3 is downstream runoff. The unique perspective offered

by space-borne radar data was used by AbuBakr et al. [7] to define structurally controlled paleo-lakes along Wadi El-Arish, which were filled during pluvial phases. The contribution of paleo-lakes and recent flash floods in recharging the shallow aquifers is significant and were dealt by many researchers [8], [9], [6], [10], [1], [11] and [5].

Yet, no specific researches involving the integrated framework of remote sensing, GIS and watershed modelling for determining optimum sites for RWH constructions, in addition to proposing their appropriate designs was performed.

Yet, no specific researches involving the integrated framework of remote sensing, GIS and watershed modelling for determining optimum sites for RWH constructions, in addition to proposing their appropriate designs was performed.

1.1 Climate

From the climate point of view, sporadic rainfall storms over Sinai hills are channelled as surface runoff through a network of minor valleys, which join into a few valleys that ultimately debouch into the Mediterranean Sea, Gulf of Suez and Gulf of Aqaba (Fig 1b). Wadi El-Arish is a dry basin, where it intercepts occasional flash floods, which run over the central carbonate plateau of Sinai towards the Mediterranean Sea. Twenty two meteorological stations, in and adjacent to Sinai Peninsula, were considered to perform the runoff calculation models (Fig. 1d). The average monthly rainfall data and Piche evaporation data were obtained from the published and non-published sources for a period of 10 years [1], [5], and the references therein. An isohyetal map of Sinai was prepared based on the mean annual rainfall (Fig. 1d). Accordingly, from El-Teeh Plateau to Gebel El-Maghara, the mean annual rainfall ranges from 22 to 40 mm/y, whereas along the southwestern coast, the rainfall ranges from 10 to 22 mm/y. Northwards and northeastwards of Gebel El-Maghara and Gebel El-Halal, the mean rainfall increases steadily, reaching 58 mm/y at Abu Aweigila and about 100 mm/y at El-Arish.

2. Material and Methods

To achieve the objectives of this research, the following tasks were performed:

2.1 Satellite image collection, preparation, processing and base map construction

The ETM+ (acquired in 2006) and SPOT-4 satellite images (acquired in 2011) were used. Both multispectral and panchromatic scenes are calibrated into geographic latitudes/longitudes, and transformed from *.dat format to *.img format through the import module of Erdas Imagine 10.1© software [12]. Subsequent to this step, it has been converted to the Universal Transverse Mercator (UTM), WGS 1984 map projection, to become compatible with the different GIS thematic layers. The bands used in SPOT-4 are blue (0.43-0.47 µm), green (0.50-0.590 µm), red (0.61-0.68 µm), near-infrared (0.79-0.890 µm) and mid-infrared (1.58-1.75 µm) [13].

A base map was constructed for the drainage basins (watersheds) of Sinai comprising the watershed boundaries as shown in Fig. 1c. The map was constructed by using the published and validated topographic maps of the Egyptian General Authority for Civil Survey [14], with multi-scales, i.e., 1:500,000 (4 sheets), 1:250,000 (11 sheets) series. Additional validation and verification were performed using Google Earth maps and Satellite ETM+ images.

A geo-database is created to hold all the map features and model primary data layers and creating relationships inside the geo-database [15]. Geostatistics uses the statistical variation as an important source of information for improving predictions of an attribute at un-sampled points, given a limited set of measurements [15]. Accordingly, geostatistics are a vital extension in the ArcGIS 10.1 software tool kit for spatial analysis.

The ETM+ (acquired in 2006) and SPOT-4 satellite images (acquired in 2011) were used. Both multispectral and panchromatic scenes are calibrated into geographic latitudes/longitudes, and transformed from *.dat format to *.img format through the import module of Erdas Imagine 10.1© software [12]. Subsequent to this step, it has been converted to the Universal Transverse Mercator (UTM), WGS 1984 map projection, to become compatible with the different GIS thematic layers. The bands used in SPOT-4 are blue (0.43-0.47 µm), green (0.50-0.590 µm), red (0.61-0.68 µm), near-infrared (0.79-0.890 µm) and mid-infrared (1.58-1.75 µm) [13].

A base map was constructed for the drainage basins (watersheds) of Sinai comprising the watershed boundaries as shown in Fig. 1c. The map was constructed by using the published and validated topographic maps of the Egyptian General Authority for Civil Survey [14], with multi-scales, i.e., 1:500,000 (4 sheets), 1:250,000 (11 sheets) series. Additional validation and verification were performed using Google Earth maps and Satellite ETM+ images.

A geo-database was created to hold all the map features and model primary data layers and creating relationships inside the geo-database [15].

2.2 Construction of drainage net map

The construction of the drainage network is the basic GIS entity to perform any hydrological calculations or runoff watershed modelling practices. In modern research methods, the reliance on digital elevation models (DEMs) and satellite imagery with high precision for the extraction of

drainage networks and the boundaries of their basins coupled with the constant stream threshold value are becoming a common practice [16], [17] and [18] DEM data treated for such a purpose has the advantage that it is easily imported, exported and analyzed by the GIS tools of the ArcGIS 10.1© software.

The task of automatic extraction of drainage network was performed inside the WMS 8.0© software platform using the "Main Drainage Module" then through its sub-modules using the TOpographic PArameteriZation program (TOPAZ) program [19]. A modified version of this program is distributed with the WMS software for the purpose of computing flow directions and flow accumulations for use in basin delineation with DEMs. However, TOPAZ is capable of further DEM elevation processing, including raster smoothing, basin and stream delineation and ordering, and development of other watershed parameters [20]. WMS 8.0© software is capable of writing an input file for DEDNM (the primary TOPAZ module).

Registered topographic maps are usually used for the validation and verification purposes and for the extraction of locations utilities or basin names. A 30-m resolution DEM has been obtained from the Advanced Space Borne Thermal Emission & Reflection Radiometer (ASTER) [21].

2.3 Runoff calculations and watershed modeling

The hydro-morphometric parameters of Wadi El-Arish watershed were determined using watershed modeling systems software (WMS 8.0©) [22], which differentiated the basins and provided multiple watershed characteristics. The watershed hydrographic criteria derived from the WMS 8.0 Software, which were used for the determination of the RWH optimum sites include: basin area (BA), basin slope (BS), basin length (BL), maximum flow distance (MFD), rock or soil infiltration (SI), volume of annual flood (VAF), average overland flow distance (OFD), total runoff and runoff loss by infiltration. These criteria were provided for each of the delineated sub-watersheds of Wadi El-Arish watershed (Table 1).

Here, the drainage frequency density (DFD) and lineament frequency density (LFD) maps were prepared by using the constructed drainage net map and by the automatic extraction of lineaments from satellite images and enhanced from geological maps. A grid system of 25 km x 25 km had been used for the construction of DFD and LFD maps, where the number of lineaments or drainage lines within each unit area of the grid was automatically counted (i.e. per 625 km^2).

Subsequently, a weighted spatial probability model (WSPM) was constructed using the prepared multi-layer GIS, to classify the study area into three gradational RWH potential areas. These layers are generated in steps, viz digitization, editing, building topological structure and finally polygonization in ArcGIS 10.1© Spatial Analyst Module [23]. The overall flowchart of methodology is given in Fig. 2.

Two runoff calculation models were used: the Soil Conservation Service Curve Number (SCS-CN) USDA SCS-CN, [24] and the Finkel, [25] methods, which were run inside the WMS 8.0© software platform [22]. However, the two methods have their advantages and disadvantages according the environmental conditions of their application. Finkel, [25] used his method for the Wadi Araba, which have similar climate conditions to Sinai Peninsula. It is a simple graphical method to determine the probability or frequency of occurrence of annual or seasonal rainfall. On the other hand, some researchers Ponce and Hawkins, 1996 [26]; Mishra and Singh, 2003 [27], and Geetha et al., 2007 [28] have pointed out limitations and cautions to the use of the SCS-CN method [24] for estimating runoff in arid regions. The concerns include the limited regional extent (Midwestern) and landscape (agricultural) in which it was developed. However, for these reasons, the authors adopted and modified the soil infiltration groups of this method to be more reliable for the Sinai arid environment [1].

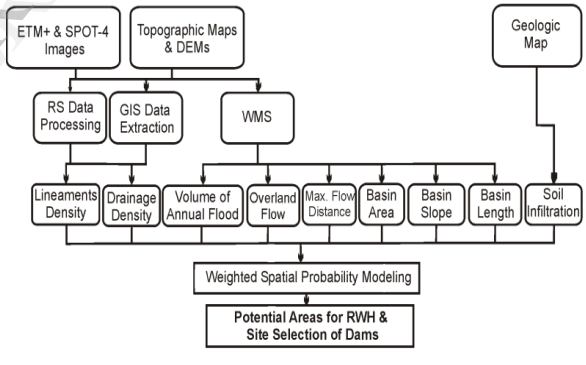

Fig. 2: Flow chart of methodology

The Finkel empirical method [25] uses the following parameters (Eqs. 1 and 2):

2.3.1 Finkel Method

1. Peak flood flow (Q_{max})

$$Q_{max} = K_1 A^{0.67} \quad [1]$$

Where Q_{max} = Peak flood flows, in m^3/sec.

2. Volume of annual flood (V) in 10^3 cubic meters

$$V = K_2 A^{0.67} \quad [2]$$

Where A is the area of the basin in km^2, and K_1 and K_2 are constants depending on probability of occurrence:

Probability of occurrence in a given year	K_1	K_2
10%	1.58	26.5

Here we used 10 % because it is very suitable for the local climate conditions.

2.3.2 SCS-CN Method

The empirically based (SCS-CN) method for estimating the volume of surface runoff was used [24]. The purpose of using the WMS 8.0© software is to calculate the peak flood discharge using the DEM and the weighted curve numbers generated from the existing land use and soil data. The major elements of the rainfall–runoff processes are embodied in the SCS-CN method [29], [30], [31] and [1], and they are: (1) catchment characteristics, (2) precipitation, evaporation, evapotranspiration, and (3) runoff. The SCS-CN method is based on the water balance equation and two hypothetical equations such as the proportional equality and linear relationship between the initial abstraction and potential maximum retention, like that in equations 3 through 7 [27]. A water balance equation is expressed as (Eq. 3):

$$P = I_a + F + Q \qquad [3]$$

and the proportional relationship is defined as (Eq. 4):

$$\frac{Q}{P - I_a} = \frac{F}{S} \qquad [4]$$

and for simplification, the following condition is defined as (Eq. 5):

$$I_a = \lambda S \qquad [5]$$

Where P = total rainfall in mm; I_a = initial abstraction; Q = excess rainfall or direct runoff volume (direct runoff depth in mm); F = cumulative infiltration excluding I_a; S = maximum potential abstraction of water by soil in mm; and λ = 0.2 (a standard value). Potential maximum retention when runoff begins, S, is expressed in terms of a scale parameter, CN, which can vary between 0-100 representing zero storage or 100 % runoff. CN is the hydrologic soil cover complex runoff curve number (non-dimensional). The value of CN is derived from the tables given in the National Engineering Handbook, Section-4 (NEH-4) [24] for the catchment characteristics, such as soil type, land use, hydrologic conditions, and antecedent soil moisture conditions. The higher the CN value the greater the runoff potential of the sub-watershed and vice versa.

$$S = \frac{25{,}400}{CN} - 254 \qquad [6]$$

Therefore, the SCS runoff equation for total runoff, Q, can be expressed as (Eq.7):

$$Q = \frac{(P - I_a)^2}{(P - I_a) + S} = \frac{(P - 0.2S)^2}{P + 0.8S} \qquad [7]$$

Where Eq. (7) is valid for $P \geq I_a$, Q = 0.

Accordingly, the present work describes a process for determining the site characteristics and developing an integrated approach including RS, GIS and WMS 8.0© software for determining the RWH potentialities and optimum sites for installing the water harvesting dams.

3. Results and Discussions

After defining basins attributes with the DEMs inside the platform of WMS 8.5© software, the developed multi criteria decision support layers should be converted into a data coverage for easier data storage and manipulation. The ranges of these input criteria (layers) used in the construction of the weighted spatial propability model (WSPM) are given in Table 2. Integration of these criteria in the GIS-based WSPM will result in the production of comperhensive maps determining the efficient sites suitable for RWH, with a number of classes.

The following is a short discussion of the nine criteria used for the construction of the WSPM maps

3.1 Volume of annual flood

The availability of an annual flood in a drainage basin is one of the most important determining parameters for the success of RWH [5]. The volume of annual flood (VAF) reflects the quantity of water available for harvesting.

In the present work, the VAF was calculated by the two previously discussed models; the Finkel [25] and the USDA SCS-CN [24]. Accordingly, Wadi El-Arish area was classified into five classes relative to the potential for the VAF generation. Figure 3a shows the classes of VAF calculated by Finkel's method, where the high-very high classes (> 3,906 m^3/y) occur mostly in the extreme northeastern and the southeastern parts of Wadi El-Arish. They include parts of the Geraia and Heridien sub-watersheds in the northeast and parts of the Yarqa Abu Taryfya sub-watershed in the southeast (Tables 1-2; Fig. 3a).

Table 1: WMS 8.0© software hydrographical output criteria used for demarcating the watersheds characteristics

Basin ID (see Fig. 1c for locations)	Wadi (Valley) name	Basin area (km^2)	Basin slope (m/m)	Basin length (m)	Overland flow Distance (m)	Max. flow distance (m)	Volume of annual flood (1000 m^3) (Finkel method)	Volume of annual flood (m^3/year) (SCS-CN method)	Total Runoff (m^3/y)	Runoff loss by infiltration (m^3/y) (SCS-CN method)	Time to peak discharge (min)
Wadi El Arish Sub-watersheds											
1	El Hamma El Hassana	3590.29	0.05988	85571	833	36902	640	16234425	28578308	12343883	1536
2	El Bruk	3299.23	0.02756	90989	837	29224	602	14304144	26653440	12349296	1535
3	Yarqa Abu Taryfya	6345.60	0.05607	138390	727	23174	495	42593062	66788359	24195297	2790
4	El Fetahy El Aqaba	2544.64	0.04140	104550	740	17908	447	14405379	25474092	11068713	1527
5	Geraia	3083.58	0.03718	81676	802	21253	571	16066820	28723209	12656389	1530
6	Heridien	3905.03	0.06372	94398	871	143023	2676	14792676	26569987	11777311	1542
7	Central W. El Arish	613.32	0.03362	46710	858	77870	2746	3098567	5558633	2460066	1535

Table 2: Ranges of input criteria used for the WSPMs

Watershed RWH Criteria	Very high	High	Moderate	Low	Very low
Basin area (Km^2)	> 4634	4633-3541	3540-2845	2844-1752	< 1751
Basin length (m)	> 97414	97413-79978	79977-72559	72558-55123	< 55122
Basin slope (m/m)	> 0.129	0.128-0.064	0.063-0.045	0.044-0.04	< 0.039
Drainage frequency density (density/625 km^2)	> 222	221-162	161-121	120-61	< 60
Lineament frequency density (segment/625 km^2)	< 3	4-6	7-13	14-29	> 30
Maximum flow distance (m)	> 176645	176644-153387	153386-139829	139828-131925	< 131924
Average overland flow distance (m)	> 1002	1001-909	908-850	849-812	< 811
Volume of annual flood (1000 m^3) (by Finkel method)	> 5105	5104-3906	3905-2707	2706-1508	< 1507
Volume of annual flood (m^3/year) (by SCS-CN method)	> 17135168	17135167-10978412	10978411-6870977	6870976-4130731	< 4130730
Soil Hydrologic Group (USDA SCS 1989)	a		b	c	d

The moderate class (2,707-3,905 m^3/y) of the VAF occurs in the central-northeast and south-southeast parts of Wadi El-Arish watershed. It is represented by parts of the Yarqa Abu Taryfya sub-watershed at the south-eastern part of W. El-Arish and parts of the Heridien, Geraia and Fetahy El-Aqaba sub-watersheds in the north-eastern parts of Wadi El-Arish watershed. The low-very low VAF classes (< 2,706 m^3/y) are encountered in the central-north-western and south-central parts of Wadi El-Arish watershed. The representative basins of these classes are El-Kharoba, El Hamma El Hassana, El Bruk, Yarqa Abu Taryfya, El Fetahy El Aqaba, Geraia and Heridien sub-watersheds.

On the other hand, little shift in the spatial distribution of the VAF classes was observed in case of the VAF map constructed by the SCS-CN method [24] (Fig. 3b), where the area occupied by the very high class (> 17,135,168 m^3/y) was shrunken to a small isolated circular area in the southern-central parts of Wadi El-Arish (i.e., a part of Yarqa Abu Taryfya sub-watershed), whereas the high class of VAF was enlarged to comprise a larger area in north-northeastern and southern-central parts of Wadi El-Arish watershed.

However, the areas of moderate-low classes occur in central and western margins of Wadi El-Arish and also at its extreme northern delta. They comprise parts of El-Bruk, El Hamma El Hassana, Yarqa Abu Taryfya, El-Feahay El Aqaba and Geraia sub-watersheds. Here, the high RWH potentiality class (17,135,167-10,978,412 m^3/y) in Fig. 3b is widned at the expense of the moderate-

low classes (4,130,731-10,978,411 m^3/y) appearing in Fig. 3a (Tables 1 and 2). This layer was assigned a weight of 12 in the WSPM (Table 3).

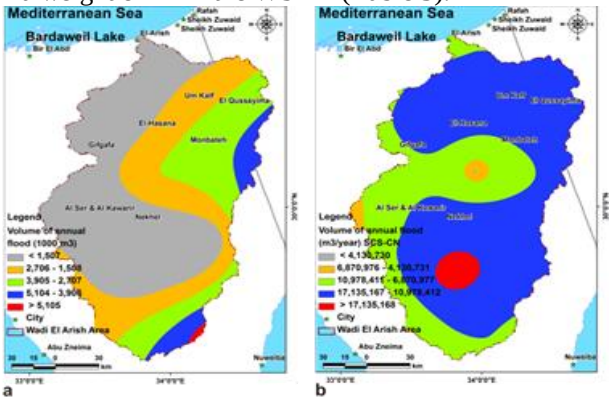

Fig. 3: GIS thematic layers used in the WSPM: VAF calculated by: a Finkel's Method [25]; b SCS-CN Method [24].

Table 3: Ranks and weights of criteria and their influencing classes used for the RWH potentiality mapping:

Data layer (Criterion)	RWH potentiality	Average rate	Weight (W_c)	Degree of Effectiveness
Volume of Annual Flood (VAF)	I (Very high) II (High) III (Moderate) IV (Low) V (Very low)	0.9 0.7 0.5 0.3 0.1	12	11.0 8.0 6.0 4.0 1.0
Average Overland Flow Distance (OFD)	I (Very high) II (High) III (Moderate) IV (Low) V (Very low)	0.9 0.7 0.5 0.3 0.1	11	10.0 8.0 6.0 4.0 1.0
Maximum Flow Distance (MFD)	I (Very high) II (High) III (Moderate) IV (Low) V (Very low)	0.9 0.7 0.5 0.3 0.1	11	10.0 8.0 6.0 4.0 1.0
Rock or Soil Infiltration (SI)	I (Very high) II (High) III (Moderate) IV (Low) V (Very low)	0.9 0.7 0.5 0.3 0.1	11	10.0 8.0 6.0 4.0 1.0
Lineament Frequency Density (LFD)	I (Very high) II (High) III (Moderate) IV (Low) V (Very low)	0.9 0.7 0.5 0.3 0.1	11	10.0 8.0 6.0 4.0 1.0
Drainage Frequency Density (DFD)	I (Very high) II (High) III (Moderate) IV (Low) V (Very low)	0.9 0.7 0.5 0.3 0.1	11	10.0 8.0 6.0 4.0 1.0
Basin Area (BA)	I (Very high) II (High) III (Moderate) IV (Low) V (Very low)	0.9 0.7 0.5 0.3 0.1	11	10.0 8.0 6.0 4.0 1.0
Basin Slope (BS)	I (Very high) II (High) III (Moderate) IV (Low) V (Very low)	0.9 0.7 0.5 0.3 0.1	11	10.0 8.0 6.0 4.0 1.0
Basin Length (BL)	I (Very high) II (High) III (Moderate) IV (Low) V (Very low)	0.9 0.7 0.5 0.3 0.1	11	10.0 8.0 6.0 4.0 1.0

3.2 Lineament frequency density

Lineament analysis for RWH potentiality mapping has a considerable importance, where the joints and fractures enhance the rock or soil infiltration or permeabilty that ultimately control the VAF. In addition, geological lineaments (fractures and faults) generally control relief, spatial distribution of drainage networks and groundwater accumulation under the influence of slope [32]. Accordingly, the higher the lineaments frequency density (LFD) is the lower the RWH potential, and vice versa. The LFD map with five classes referring to the number of cracks in each unit area was constructed. The five LFD classes were < 3, 4-6, 7-13, 14-29 and > 30 lineament/625 km^2, for the very high, high, moderate, low and very low potentiality for the RWH, respectively (Fig. 4a; Table 2). The High to very high LFD classes (> 14/625 km^2) are encoutered within the fractured carbonate rocks of central Sinai, with some localized areas of high class occurring in northwest, norteast and western parts of Wadi El-Arish watershed, whereas the density decreases away from this territory towards north and south (Fig. 4.a). This layer was rated a weight of 11 in the WSPM (Table 3).

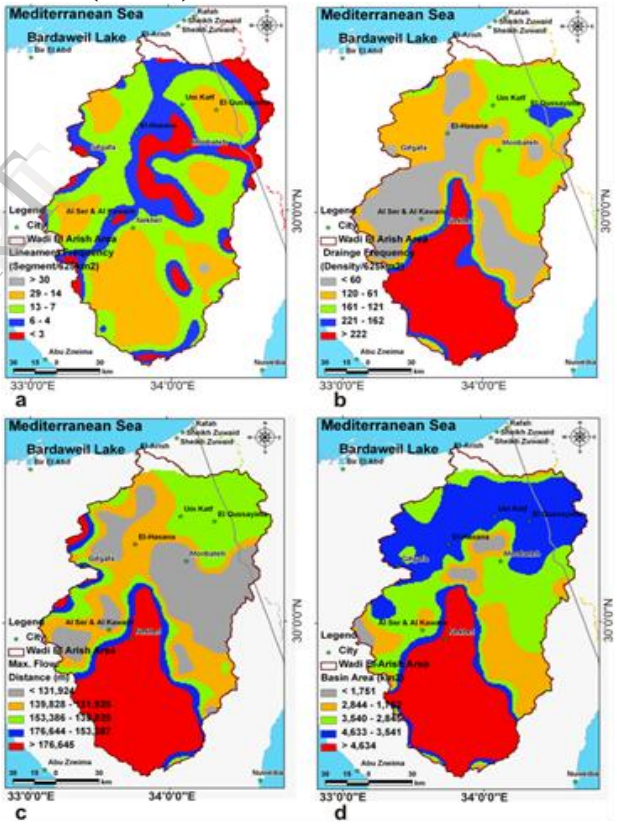

Fig. 4: GIS thematic layers used in the WSPM: a LFD; b DFD; c MFD; d BA

3.3 Drainage Frequency Density

The drainage frequency density (DFD) is a measure for the degree of fluvial dissection and is influenced by numerous factors, among which, the resistance to erosion of rocks, infiltration capacity of the land and climate conditions [33]. The higher the DFD is the higher the RWH potential, and vice

versa. The DFD five classes were ordered as: > 222, 221-162, 161-121, 120-61, > 60 segment/625 km^2, for very high, high, moderate, low and very low for RWH, respectively (Tables 2; Fig. 4b). This layer had been assigned a weight of 11 in the WSPM (Table 3).

3.4 Maximum Flow Distance

The Maximum Flow Distance (MFD) of a basin includes both overland and channel flow [34] (Tables 1-2; Fig. 4c). It is the maximum length of water's path in the drainage basin (m). This factor is important in determining the RWH capability of a drainage basin, as the higher the MFD the higher the RWH possibilities.

It is also a function of the basin area. The constructed thematic map of the MFD criterion indicated that the very high-high classes occupy the southern-central and the extreme western parts (Yarqa Abu Taryfya and small strip at the western flanks of El Bruk and El-Hamma El-Hassana subwatersheds) with a maximum flow distance ranges from 153,387 to more than 176,645 m (Table 2). The very low class of the MFD is encountered in the central-eastern parts of Geraia sub-watershed and some small parts in El-Bruk, El-Hamma El-Hassana, and El-Fatahay El-Aqaba sub-watersheds. The low to moderate classes (131,925-153,386 m) occupy the greater parts of the study area with the largest area of moderate MFD class occurring at the northwestern parts (i.e. Heridien sub-watershed) (Fig. 4c; Tables 1-2). This layer had been rated a weight of 11 in the WSPM (Table 3).

3.5 Basin Area

Basin area (BA) is defined as the total area in square kilometers enclosed by the basin boundary [34]. Basin area had been identified as the most important of all the morphometric parameters controlling the catchment runoff pattern. This is because, the larger the size of the basin, the greater the amount of rain it intercepts and the higher the peak discharge that result [35] and [33] (Table 1). Another reason for the high positive correlation between basin area and the discharge is the fact that the basin area is also highly correlated with some of the other catchment hydromorphometric characteristics which influence runoff, such as basin length (i.e. the larger the basin, the longer its length), average overland flow distance and maximum flow distance [37] and [38].

The thematic layer for BA with five classes was generated (Fig. 4d). The very high basin area class (> 4,634 km^2) occurs in one of Wadi El-Arish upstream sub-watersheds (i.e. Yarqa Abu Taryfya) with a 6345.6 km^2. The high-moderate basin area classes (4633-2845 km^2) are represented by the northern and central sub-watersheds (i.e. Heridien and El-Hamma El-Hassana) (Table 2). The low basin area class (2844-1752 km^2) is represented by the El-Fetahy El-Aqaba sub-watershed, which occurs in the southeastern part of Wadi El-Arish watershed. This layer was assigned the weight of 11 in the WSPM (Table 3; Fig. 4c).

3.6 Basin Slope

Slope plays a very significant role in determining infiltration versus runoff. It plays a very strong role in determining rainwater deceleration, acceleration or infiltration [39]. The slope of the drainage basin is a key factor for the selection of water harvesting locations in order to get the maximum storage capacity in the channel. It is the average slope of the triangles comprising this basin [34] and [40]. Reasonable care should be taken in determining this parameter as peak discharge and hydrograph shape are sensitive to the value used for basin slope [41].

In the present work, slope map is generated from the DEM. Five slope classes were generated. The slope map was merged with the basin map to create slope attributes of each drainage basin. The thematic layer of BS indicates an increase in value due south in the mountainous terrains in El-Teeh and Egma Plateau (slope > 0.064) (Fig. 5a; Tables 1-2). Whereas, the BS decreases in the central (<0.044), which doubles the possibilities of RWH. The possibility of RWH is higher in gentle or medium-sloped basins of central–southern and northern wadies of El-Arish watershed (0.063-0.045). This layer was assigned the weight of 11 in the WSPM (Table 3; Fig. 5a).

3.7 Basin Length

The basin length (BL) is defined as the distance which cut the basin into two similar parts [34]. The longer the BL, the lower the chances that such a basin will be flooded, if compared with a more compacted basin like those occurred in Central Wadi El-Arish sub-watershed (Fig. 5b). This is because, the longer the basin, the lower its slope and hence the higher the possibilities for RWH (Table 1). Micro catchment RWH techniques are more successful in shorter basin lengths, whereas macro catchment procedures are more applicable in longer basin lengths, which characterize the sub-watersheds of Wadi El-Arish (Tables 1-2). This layer was assigned a weight of 11 in the WSPM (Table 3; Fig. 5b).

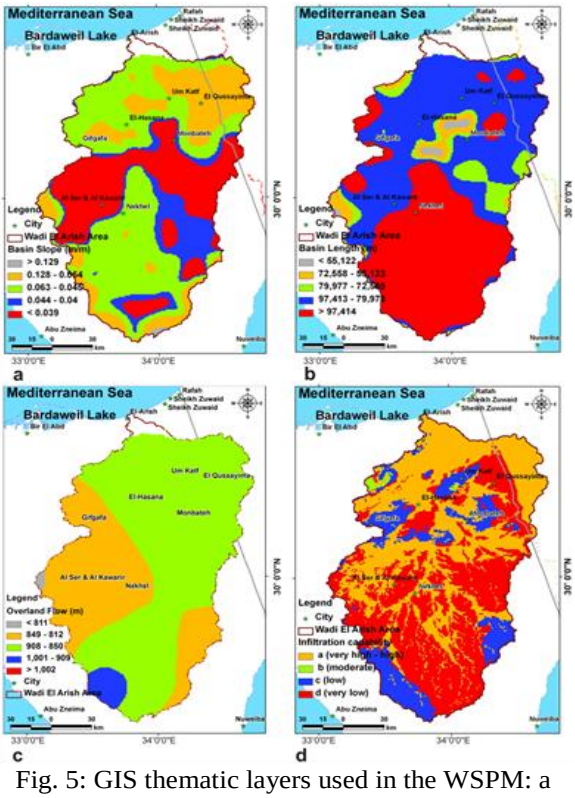

Fig. 5: GIS thematic layers used in the WSPM: a BS; b BL; c OFD; d SI

3.8 Average Overland Flow Distance

The average overland flow distance (OFD) within the basin is computed by averaging the overland distance traveled from the centroid of each triangle to the nearest stream. The overland flow is the water that flows over the slopes of the drainage basin and is then concentrated into stream channels. When rainfall is called surface runoff when reaches the channel. Also, it is known as surface flow [34]. Most of Wadi El-Arish watershed is represented by the moderate class of the OFD (850-849 m), with varying reliefs and slopes, which determine where overland is effective and generated. It is also affected by the type of soil lithology of surface topography, which governs the erosion rates by overland flow [42]. The thematic layer of the OFD indicates a pronounced decrease in the western and southeastern parts (812-849 m) (low class), which were occupied by parts of the Yarqa Abu Taryfya, El Bruk and El Hamma El Hassana sub-watersheds and parts of the Fetahay El Aqaba sub-watershed in the southwestern part of W. El-Arish main watershed (Fig. 5c; Tables 1-2). The very low OFD classes (< 811 m) are encountered only in a very small area in the western part of W. El-Arish watershed. The moderate class of OFD (850-908 m) is occupied by the Central Wadi El Arish, El-Hamma El Hasana, Heridien, Geraia, El Fetahy El Aqaba and Yarqa Abu Taryfya sub-watersheds. However, this map reflects the effect of soil infiltration of the sub-terrain, where the segregation of Wadi El-Arish watershed into different classes with different infiltration capabilities (Fig. 5d) gave good reasons behind the spatial distribution of the OFD. Accordingly, the low OFD occurs in areas characterized by very high and high infiltration capability and vice versa (Figs. 5c and 5d). This layer was assigned a weight of 11 in the WSPM (Table 3; Fig. 5c).

3.9 Soil Infiltration

Infiltration is one of the main factors influencing the flash floods and their energy. It is the process by which precipitation is abstracted by seeping into the soil below the land surface [43]. The layer of soil infiltration (SI) is essential to understand the nature and distribution of infiltration capabilities of surface rock units [44]. The SI determines whether the water will infiltrate or rather runoff over the soil surface.

The classification of lithologic formations according to their infiltration capabilities was carried out depending on the intensive previous investigations or previous work (NARSS, 2009 [45] and the references therein), in addition to the Soil Groups based on the USDA soil classification scheme [24] (Table 2). Thus, a map with four classes was produced to reveal rock formations of similar infiltration properties or lithological groups a, b, c and d. According to these groups, infiltration rates decreases from a to d, which is inversely related to the RWH capabilities for the same group. The higher the infiltration capability of the soil is the lower the RWH potentialities, and vice versa. In the obtained classification, soil or rock groups of similar hydrologic properties representing the study area were embedded in one map (Fig. 5d). The classified map with four classes was used instead of the five classes, as the SI class a includes both high and very high infiltration capabilities. This layer was assigned a weight of 11 in the WSPM (Table 3).

3.10 Weighted Spatial Probability Modeling

The multi-criteria decision support system (MCDSS) [46] represented by the previously discussed nine thematic layers, were ranked according to their magnitude of contribution to the RWH, thus they were categorized from very high to very low contribution and the same classes were used in the RWH potentiality mapping (Table 3; Fig. 6a-b). Two weighted spatial probability models (WSPMs) were generated, where the model was run twice; one with the VAF calculated by Finkel and the other by the SCS-CN runoff models. The models' running implied the integration of all criteria as thematic layers in the WSPM. Accordingly, two output maps will be obtained by the WSPM with a number of classes indicating the categories of RWH potentiality (i.e. high, moderate

and low). However, all the previously discussed criteria have the same magnitude of contribution on RWH potentiality, except the criterion of VAF, which have a relatively higher weight of contribution on the RWH, as it represents the actual expected available runoff water for harvesting (Table 3). However, some criteria work positively while others work negatively in RWH potentiality mapping. Accordingly, the BS, LFD and SI criteria work negatively in RWH, whereas the VAF, OFD, BA, BL, DFD and MFD work positively.

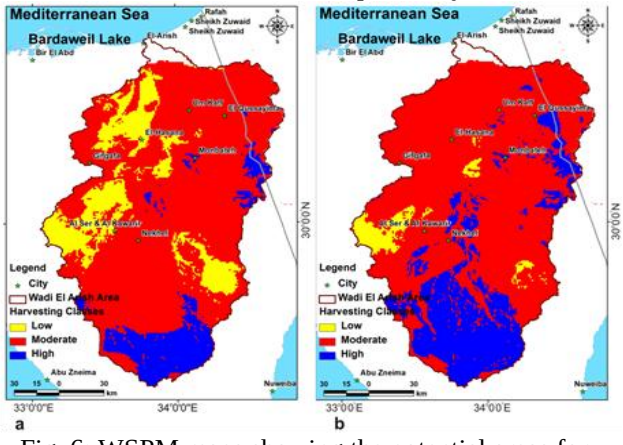

Fig. 6: WSPM maps showing the potential areas for RWH in W. El-Arish in two scenarios: a: when VAF was calculated by the Finkel's method; b: when the VAF was calculated by the SCS-CN method

The weights and rates were assumed and optimized for the MCDSS depending on the experience or judgments of the authors and the opinions of experts in the previous similar works on RWH potentiality mapping (i.e., the qualitative methods performed by Adiga and Krishna Murthy [47]; Anbazhagan et al. [48], in addition to the geostatistical normalization and cross-validation (quantitative methods) within the ArcGIS 10.1© platform before running the model [49]. The cross validation (CV) is a statistical procedure for testing the quality of a predicted data distribution and the model results. The CV removes one data location then predicts the associated data using the data at the rest of the locations. The primary use for this tool is to compare the predicted value to the observed value in order to obtain useful information about some of the model parameters [23]. The weights and rates were determined depending on the magnitude of contributions between each layer range of the WSPM classified layers. Accordingly, the integrated criteria were given a weight of 11 except for the VAF, which was assigned a weight of 12%. After proposing criteria weights, categorization was applied to each of the five classes among each criterion. For example, the classes graded from I (very high potential) up to V (very low potential) according to their importance in the RWH potentiality mapping (Table 3).

Taking 100% as a maximum value for the rank, thus for the five classes, ranks will be classified as 100-80, 80-60, 60-40, 40-20 and 20-0%, respectively. Consequently, the average of ranking for each class will be 0.90, 0.70, 0.50, 0.30 and 0.10% for classes from I-V, respectively (Table 3).

Table 4: Areas of RWH potentiality classes

Harvesting potentiality map (VAF calculated by Finkel 1979 method)			
RWH Potentiality class	**Low**	**Moderate**	**High**
Area (Km^2)	3617.51	17234.42	2511.78
Area (% of the total study area) Total study area: 23369.97 Km^2	15.48	73.75	10.77
Harvesting potentiality map (VAF calculated by USDA SCS-CN 1989 Method)			
RWH Potentiality class	**Low**	**Moderate**	**High**
Area (Km^2)	842.80	17462.11	5065.81
Area (% of the total study area) Total study area: 23369.97 Km^2	3.61	74.72	21.68

The degree of effectiveness (E) for each thematic layer was calculated by multiplying the criterion weight (W_c) with the criterion rank (R_c). For example, if the weight of VAF equals 12% and this is multiplied by the average rank of 90 (for class I), the degree of effectiveness will be 11 (Eq. 8).

$$E = W_c \times R_f = 0.12 \times 90 = 11 \quad [8]$$

According to this method of data manipulation, the assessment of the effectiveness of each decision criterion provides a comparative analysis among the different thematic layers. Therefore, it is clear from Table 3 that class I in the VAF criterion (i.e., E =11) represents the most effective criterion with regard to the RWH potentiality mapping, compared to the least influencing class V (i.e., E=1) in all criteria.

Therefore, an arithmetic overlay approach built into ArcGIS 10.1© Spatial Analyst Model Builder was carried out for performing the WSPM. This overlay processing manipulates both continuous and discrete grid layers and the derived data are continuous grid data layer. Two WSPM output maps for RWH potentiality with four classes ranging from very low to high potentiality were obtained.

The spatial distribution of these classes relative to the total area studied is: 15.48 (low), 73.75 (moderate) and 10.77 % (high) for the RWH potentiality map constructed by using the VAF that was calculated by the Finkel's method (Fig. 6a;

Table 4), and as: 3.61 (low), 74.72 (moderate), and 21.68 % (high), for the map constructed by using the VAF which was calculated by the USDA-SCS-CN method (Fig. 6b; Table 4). From these two WSPM output maps, it is clear that there is a good correlation between them.

From these WSPM maps, it could be concluded that the major area of Wadi El-Arish watershed is categorized as of moderate RWH potentiality (73.75-74.72 % of total wadi area), especially, in its central and northern parts. As previously discussed, the southern parts of Wadi El-Arish, the DFD is moderate-very high (>121/625 km^2), which is noticeably decreasing to the central and northern reaches of the wadi (<121/625 km^2).

This spatial variation and decreasing in magnitudes of DFD due north, also confirms the variation in soil infiltration (SI) capability, where significant low-very low values of SI are revealed in the southern and central portions of the wadi in contradiction to the northern ones. Such clues advocate the central-southern areas of Wadi El-Arish watershed as optimum for the RWH.

3.11 Proposing optimum sites for the RWH control works and minimizing environmental hazards

The previous discussions led to the suggestion of two surface storage dams connected with each other's via a specific canal, which in turn, are connected to the Rawafaa Dam with an artificial conveying canal as shown in the location map (Fig. 7a). These dams (Dams nos. 1 & 2) will be able to store the annual flood water to achieve a steady perennial water flow to service the developmental activities in central Sinai. As a positive impact, the suggested two dams will rise the operational lifetime of the elderly El-Rawafaa Dam located to about 70 km north of dam no. 2. This improvement will be achieved by decreasing the rates of siltation upstream the Rawafaa Dam, where it is currently suffer from this phenomenon. The Rawafaa dam is an arched masonry located in Wadi Al-Arish, at about 52 kilometres south of El-Arish City.

This dam was built in 1946 and reportedly had an initial capacity of about 3 million cubic meters [50], [51] and [52] also provided data indicating that the dam was reduced in capacity from 3.03 x 10^6 m^3 in 1949 to 2.94 x 10^6 m^3 in 1958; including an average loss of capacity of only 10,000 m^3/y.

From the results of the present work, the criteria used for the site selection of proposed dams include:

- Collection of runoff water at the outlets Wadi El-Arish upstream sub-watersheds, which are characterized by adequate VAF (i.e., El-Bruk: 14,304,144 m^3/y; Yarqa Abu Taryfya: 42,593,062 m^3/y; El-Fetahay El-Aqaba: 14,405,379 m^3/y; Geraia: 16,066,820 m^3/y).
- The results of the WSPM for determining RWH potentialities (in high and moderate classes).
- The soil characteristics, which will provide the good environment for agriculture (alluvial or wadi deposits).
- Existing land use pattern, which should be outside the present inhabited areas. The harvested runoff water will provide new areas suitable for the settlement of new communities.
- Surface topography in terms of side slopes, which provide shoulders for the proposed dams to maintain a reasonable stability for the installed proposed dams.

The successful design, construction and operation of a reservoir project of a dam over a full range of loadings require a comprehensive site characterization, detailed design of each feature and continuous evaluation of the project features during operation [53].

The proposed dams were aligned with respect to their heights to be straight or of the most economical alignment fitting to the topography and founding conditions. Additionally, the dams were designed to satisfy the basic design criteria of crest levels, minimum top widths, in addition to the basic technical and administrative requirements of an embankment dam to meet the dam safety requirements (i.e. dam foundation, abutments stability under all static or dynamic loading conditions, seepage control, freeboard, spillway and outlet capacity, etc.) [54].

The two proposed dams in Wadi El-Arish are embankment dams of the rock-fill type. The rock-fill dams are classified and configured into few groups according to the dam sections [55]. In the present case, the selected dam of rock-fill type consists of various layers of rock materials with an inclined core of impervious materials.

The main body of the rock-fill dams, which should have a structural resistance against failure, consists of rock-fill shell and transitional zones, core and facing zones, which have a role to minimize the leakage through the embankment. Filter zone should be provided in any type of rock-fill dams to prevent loss of soil particles by the expected erosion resulting from the seepage flow through the embankment.

The first proposed dam no. 1 is located at the upstream of W. El-Arish basin at the mouse of three sub-basins: El-Fetahay-El-Aqaba, Yarqa Abu Taryfya and El-Bruk. The second proposed dam no. 2 is located at the mouse of Geraia sub-watershed.

Proposed dam no. 1

This proposed dam is located between latitude/longitude 585398.25 - 3347517.81 and latitude/longitude 584757.38 - 3347523.44

(kilometric coordinates) (Fig. 7a-b).The design criteria of dam no.1 include: dam length of 650 m, dam width of 10 m, side slope of 1:1, allowable dam height of 15 m, base level of 293.5 m and storage capacity of 525,000 m^3.

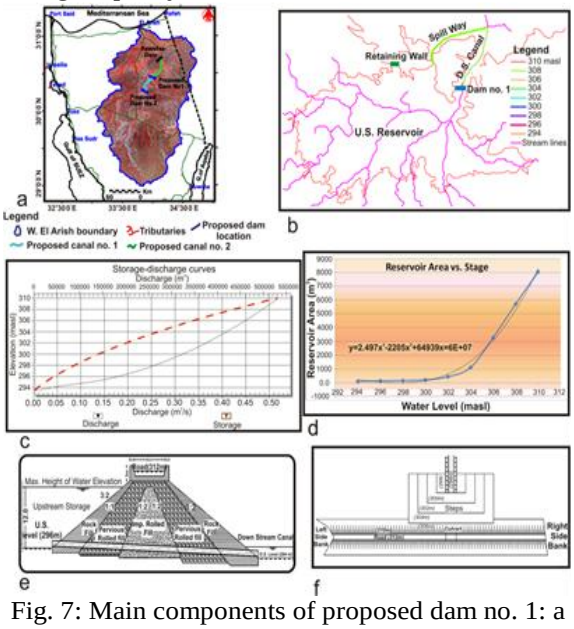

Fig. 7: Main components of proposed dam no. 1: a locations map of dams; b location map for the proposed dam no. 1 with its upstream reservoir, spillway, downstream canal, and its retaining wall; c Graph showing the water level in the reservoir formed upstream the dam vs. the volume of water stored and released from the reservoir relative to the water head; d Relationship between the water stored upstream the dam vs. water level stages; e typical cross-section in the proposed dam; f Typical plan of the dam

Fig. 7a-b shows the location of proposed dam no. 1 with its upstream reservoir, spillway, downstream canal, and its retaining wall. Figure 7.c shows the volume of water that could be stored upstream of the first proposed dam no. 1 versus the storage height. Furthermore, it shows the water flow downstream the proposed dam through a pipe, with a diameter of 0.6 m with an inclination of 0.02.

Figure 7d illustrates the area of water stored upstream the proposed dam no.1 vs. variable water level stages. Figures 7e-f show the typical longitudinal cross sections and plan views of the proposed dam no. 1 and showing the left and right shoulders and the downstream steps, which prevent the downstream scouring and achieve safe water over flow, if the upstream water level reach its maximum limit. Also, the figures show the downstream open canal.

Proposed dam no. 2

This proposed dam is extending from latitude/Longitude 597337.20-3368480.54 to latitude/Longitude 596878.06-3368485.64 (Figs. 7a and 8.a).The design criteria of dam no.2 includes: dam length of 500 m, dam width of 10 m, side slope of 1:1, allowable dam height of 15 m, base level of 237 m, storage capacity of 250,000 m^3.

Figure 8.b shows the volume of water that can be stored upstream of the second proposed dam no. 2 versus the storage height. Figure 8c shows the area of stored water upstream the proposed dam no. 2 with variable water level stages. Furthermore, the figure shows the flow downstream the proposed dam through a pipe with a diameter of 0.6 m, which has an inclination of 0.02 (Fig. 8d).

Figures 8d through 8g show typical cross sections and plan views of the proposed dam no. 2, the left and right dam shoulders and the downstream steps, which prevent the downstream scouring and achieve safe water over flow, if the upstream water level reaches its maximum limit. In addition, these figures show the downstream open canal, typical views for the retaining wall, upstream reservoir spill way and typical cross sections in the retaining wall and spill way for the upstream reservoir of dam no.2.

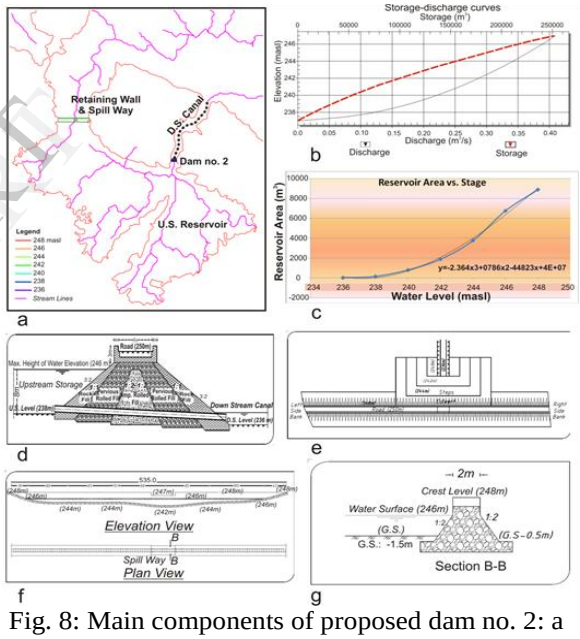

Fig. 8: Main components of proposed dam no. 2: a Location of the dam showing its upstream reservoir, spillway, downstream canal and retaining wall; b Storage-discharge curves; c Relationship between water stored upstream the dam with different water stages; d typical cross-section in the dam; e Typical plan for the dam; f typical views of the retaining wall and spillway for the upstream reservoir; g typical cross-section in the retaining wall and spillway for upstream reservoir of the dam

4. Summary and Recommendations

Remote sensing, watershed modelling and GIS techniques are modern research tools that proved to be highly effective in mapping, investigation and modeling the runoff processes and optimization the runoff water harvesting (RWH). In the present

work, these tools were used to determine the potential sites or areas suitable for the RWH in W. El-Arish Watershed. The performed weighted spatial probability models (WSPMs) segregated the watershed into three potential classes for the RWH, which are graded from low to high. The two performed WSPMs (Finkel's and SCS-CN) ellucidated that the areas of high potentiality for RWH are occupying only 10.77-21.68 % (or 2511.78-5065.8 Km^2, respectively), whereas the areas of low potentiality for the RWH are occupying 15.48-3.61% (or 3617.50-842.80 Km^2, respectively). However, most of W. El-Arish area (73.75-74.72 %) (Or 17234.42-17462.11 km^2, respectively) is represented by the moderate potentiality class. Promising upstream sub-watersheds of W. El-Arish, which are characterized by high and moderate RWH potentiality, were selected for the collection of runoff water at their outlets. These sub-watersheds are characterized by adequate volume of annual flood (VAF) and are represented by El-Bruk: 14,304,144 m^3/y; Yarqa Abu Taryfya: 42,593,062 m^3/y; El-Fetahay El-Aqaba: 14,405,379 m^3/y; Geraia: 16,066,820 m^3/y. Two surface storage dams of rock-fill type, which are connected with each other's and with the elderly Rawafaa Dam with artificial conveying canals, were proposed. These dams will achieve perennial agricultural development in the central part of Wadi El-Arish. Design criteria, capacities and reservoirs' areas of these dams were given. Last but not least, RWH could be used as a tool for flash flood hazard mitigation at the downstream by impounding water in some places upstream the wadi.

5. Acknowledgement

The authors wish to express their great gratitude to the Science & Technology Development Fund (STDF) for kindly funding and supporting the present project. Deep gratitude is also dedicated to the National Authority for Remote Sensing and Space Sciences (NARSS) for providing the facilities needed for conducting the present work.

6. References

[1] Elewa H.H., Qaddah A.A., (2011) Groundwater potentiality mapping in the Sinai Peninsula, Egypt, using remote sensing and GIS-watershed-based modeling. *Hydrogeology Journal*, 19 (3): 613-628. (DOI 10.1007/s10040-011-0703-8).

[2] UNESCO, (1977) Map of the world distribution of arid regions. MAB Technical Notes 7.

[3] Shatta A., Attia F., (1994) Environmental Aspects of Water Harvesting. In: FAO, Water Harvesting For Improved Agricultural Production. Expert Consultation, Cairo, Egypt 21-25 Nov. 1993, p. 257-270, FAO, Rome.

[4] El-Shafei S. (1994) Agricultural Development in the North-West Coastal Zone, Egypt. Report on Water Harvesting. In: FAO, Water Harvesting For Improved Agricultural Production. Expert Consultation, Cairo, Egypt 21-25 Nov. 1993, FAO, Rome.

[5] Elewa H.H., Qaddah A.A., El-Feel A.A. (2012) Determining Potential Sites for Runoff Water Harvesting using Remote Sensing and Geographic Information Systems-Based Modeling in Sinai. American Journal of Environmental Sciences, Science Publications, USA, 8 (1): 42-55

[6] Gheith H.M., Sultan M.I., (2001) Assessment of the renewable groundwater resources of Wadi El-Arish, Sinai, Egypt: Modeling, remote sensing and GIS application. Remote Sensing and Hydrology 2000 (Proceedings of a symposium held at Santa Fe, New Mexico, USA, April 2000). IAHS Publ. no. 267, 2001.

[7] AbuBakr M, Ghoneim E, El-Baz F, Zeneldin M, Zeid S (2013) Use of radar data to unveil the paleolakes and the ancestral course of Wadi El-Arish, Sinai Peninsula, Egypt. Geomorphology 194: 34-45.

[8] El-Baz, F., Kusky, T.M., Himida, I., Abdel-Mogheeth, S., (1998) Ground Water Potential of the Sinai Peninsula, Egypt. Ministry of Agriculture and Land Reclamation, Cairo (219 pp.).

[9] Kusky, T.M., El-Baz, F. (2000) Neotectonics and fluvial geomorphology of the Northern Sinai Peninsula. Journal of African Earth Sciences 31: 213–235.

[10] Smith, S., El-Shamy, I., Abd-El Monsef, H. (1997) Locating regions of high probability for groundwater in the Wadi EI-Arish Basin, Sinai, Egypt. Journal of African Earth Sciences 25: 253–262.

[11] Sultan, M., Metwally, S., Milewski, A., Becker, D., Ahmeda, M., Sauck, W. Soliman, F., Sturchio, N., Yane, E., Rashed, M.,Wagdy, A., Becker, R.,Welton, B. (2011) Modern recharge to fossil aquifers: geochemical, geophysical, and modeling constraints. Journal of Hydrology 403: 14–24.

[12] Leica Geosystems GIS & Mapping, LLC (2008) ERDAS Field Guide, Volume 1. Norcross, GA: Leica Geosystems Geospatial Imaging, LLC.

[13] Lillesand T.M., Kiefer R.W., Chipman J.W., (2004) Remote sensing and image interpretation. 5th edition, Wiley, India (p.)Ltd., New Delhi.

[14] EGACS (1989) Egyptian General Authority for Civil Survey. Topographic sheets, scales 1:500000-1:250000.

[15] Burrough. P.A., McDonnel, R.A. (1998) Principles of geographic information systems, Oxford, Oxford Univ. Press, 330 pp.

[16] Mark D.M., (1984) Automatic detection of drainage networks from digital elevation models. Cartographica, 21(2/3):168-178.

[17] Garbrecht J., Martz L.W., (1997) TOPAZ: An automated digital landscape analysis tool for topographic evaluation, drainage identification, sub-watershed segmentation and sub catchment parameterization; TOPAZ Overview, U.S. Department of Agriculture, Agricultural Research Service, Grazing lands Research Laboratory, El Reno, OK, USA, ARS Publication No. GRL 97-3.

[18] Wen-Tzu Lin, Wen-Chieh Chou, Chao-Yuan Lin, Pi-Hui Huang and Jing-Shyan Tsai (2006) Automated suitable drainage network extraction from digital elevation models in Taiwan's upstream watersheds. Hydrological Processes, Vol. 20 (2): pages 289–306. DOI: 10.1002/hyp.5911.

[19] Lacroix MP, Martz LW, Kite GW, Garbrecht J. (2002) Using digital terrain analysis modeling techniques

for the parameterization of a hydrologic model. Environmental Modeling & Software 17: 127–136.
[20] Green, J.I., Nelson E. J. (2002) "Calculation of time of concentration for hydrologic design and analysis using geographic information system vector objects," Journal of Hydroinformatics, Vol. 4, No. 2, pp. 75-81.
[21] Rabus B., Eineder M., Roth A., Bamler R., (2003) The shuttle radar topography mission- a new class of digital elevation models acquired by space-borne radar, Photogram. Rem. Sens., 57: 241-262.
[22] AQUAVEO (2008) Water modeling solutions. Support forum for sub-watershed modeling system software (WMS) www.aquaveo.com
[23] ESRI (2007) ArcGIS 9.2® Software and user manual. Environmental Systems Research Institute, Redlands, California 92373-8100, USA. http://www.esri.com
[24] USDA-SCS-CN (United States Department of Agriculture-Soil Conservation Service-Curve Number), (1989) Estimating runoff and peak discharges. Chapter 2: in Engineering Field Handbook. http://www.info.usda.gov/CED/ftp/CED/EFH-Ch02.pdf (page accessed on August 20, 2012).
[25] Finkel H.H., (1979) Water Resources in Arid Zone Settlement, A Case Study in Arid Zone Settlement, the Israeli Experience, G. Colany ed., Pergamon.
[26] Ponce V.M., Hawkins R.H., (1996) Runoff curve number: Has it reached maturity? Hydrol. Eng. ASCE 1 (1):11–19.
[27] Mishra S.K., Singh V.P., (2003) Soil Conservation Service Curve Number (SCS-CN) Methodology. Kluwer Academic Publishers, ISBN 1-4020-1132-6, P.O. Box 17, 3300 AA Dordrecht, The Netherlands, 2-4.
[28] Geetha K., Mishra S.K., Eldho T.I., Rastogi A.K., Pandey R.P., (2007) Modifications to SCS-CN method for long-term hydrologic simulation. Journal of Irrigation and Drainage Engineering 133(5): 475-486.
[29] Hogarth W.L., Rose C.W., Parlange J.Y., Sander G.C., Carey G., (2004) Soil erosion due to rainfall impact with no inflow: a numerical solution with spatial and temporal effects of sediment settling velocity characteristics. J. Hydrol. 294:229–240
[30] Jain M.K. Kothyari U.C. Ranga Raju K.G., (2005) Geographic information system based distributed model for soil erosion and rate of sediment outflow from catchments. J. Hydraulic Eng. ASCE 131 (9): 755–769.
[31] Tyagi J.V., Mishra S.K., Ranvir Singh, Singh V.P., (2008) SCS-CN based time-distributed sediment yield model. Journal of Hydrology, El sevier. 352 pp. 388-403
[32] Gerrard A.J., (1981) Soils and landforms. An integration of geomorphology and pedology. George Allen and Unwin, London, 219 pp.
[33] Verstappen H., (1983) The applied geomorphology, International Institute for Aerial Survey and Earth Science (I.T.C.), Enschede, Netherlands, Amsterdam, Oxford, New York.
[34] Horton R.E., (1945) Erosional development of stream and their drainage basins; hydrophysical approach to quantitative morphology. Geological Society of America Bulletin, V. 56: 275-370.
[35] Morisawa M.E., (1959) Relation of morphometric properties to runoff in the Little Mill Creek, Ohio Drainage Basin, (Columbia University, Dept. of Geol.) Technical Report, 17, office of Naval Research, Project NR 389-042
[36] Pitlick, J., (1994) Relations between Peak flows, Precipitation and Physiography for Five Mountainous Regions in Western U.S.A., Journal of Hydrology, 158: 219-240.
[37] Gregory K.J., Walling D.E., (1973) Drainage Basin Form and Process: A Geomorphological Approach, Edward Arnold, London, 456 pp.
[38] Jain V., Sinha R., (2003) Evaluation of Geomorphic Control on Flood Hazard Through Geomorphic Instantaneous Unit Hydrograph. Current Science, 85(11), 26-32.
[39] Subba Rao N., (2006) Groundwater potential index in a crystalline terrain using remote sensing data. Environ Geol, 50:1067-1076. DOI 10.1007/s00254-006-0280-7.
[40] Leopold L. B., Maddock T., (1953) The hydraulic geometry of stream channels and some physiographic implications: U.S. Geol. Survey Prof. Paper 252, 52 p.
[41] Jones, J.A.A., (1999) Global Hydrology: Processes, Resources and Environmental Management, Longman, 399 pp.
[42] Montgomery D.R., Dietrich W.E., (1989) Source areas, drainage density, and channel initiation, Water Resources. Research. 25:1907–1918
[43] Ponce V.M., (1989) Engineering Hydrology, principles and practices. Prentice-Hall, Englewood Cliffs, New Jersey.
[44] Fetter C.W., (1994) Applied hydrogeology, 3rd edn. Prentice Hall, Upper Saddle River, NJ, 691pp.
[45] NARSS (2009) Surface Water/Groundwater Potentialities of Sinai Peninsula: Determining Parameters of Sustainability Using Remote Sensing & GIS Techniques. Unpublished Report .
[46] Malczewski J., (1996) A GIS-based approach to multiple criteria group decision-making. International Journal of Geographic Information Systems 10(8): 955–971.
[47] Adiga S., Krishna Murthy Y.V.N. (2000) Integrated sustainable development of land and water resources using space technology inputs. Space Forum 5(1–3) pp. 179–202.
[48] Anbazhagan S., Ramasamy SM, Das Gupta S (2005) Remote sensing and GIS for artificial recharge study, runoff estimation and planning in Ayyar basin, Tamil Nadu, *India. Environ Geol* 48:158–170. doi:10.1007/s00254-005-1284-4.
[49] Isaaks E.H., Srivastava R.M., (1989) An introduction to applied geostatistics. Oxford University Press, New York, 561 pp.
[50] Dames and Moore (1985) Sinai development study. Phase 1, The land and the environment of Sinai, Final Report submitted to the Advisory Committee for Reconstruction, Ministry of Development, Egypt. USAID Grant No. 263-0113.
[51] Shata, A., (1968) Concrete and masonry dams in Sinai, memorandum (Cairo: Dames & Moore, 1981)
[52] Taha A.H., (1968) Geology of the groundwater supplies of El-Arish-Rafaa area (North East Sinai, U.A.R., M.Sc. Thesis, Cairo U., Egypt.
[53] Mcmahon J. R., (2004) General design and construction considerations for earth and rock-fill dams, Department of the Army, U.S. Army Corps of Engineers, Washington, pp. 2-1 – 2-8.
[54] Greimann B., (1987) Design of small dams, 3rd Edition, United States Department of the Interior, Bureau of Reclamation, a water resources technical publication: pp. 287-312
[55] Kunitomo, N., (2000) Design and construction of embankment dams, Dept. of Civil Eng., Aichi Institute of Technology, pp. 2-5